



## DETECTION OF CARDIOVASCULAR DISEASES IN ECG IMAGES USING MACHINE LEARNING AND DEEP LEARNING METHODS

Prof. (Dr.) Rashed Sarkar <sup>1</sup>, Abedin Saleem Javed <sup>2</sup>, Hillol Jyoti Sarmah <sup>3</sup>, Hrishiraj Gogoi <sup>4</sup>

Computer Science and Engineering, Royal School of Engineering Technology, The Assam Royal Global University

### Abstract

Cardiovascular diseases (heart diseases) are the essential driver of mortality worldwide. The sooner they can be expected and classified, the more noteworthy the quantity of lives that can be saved. An electrocardiogram (ECG) is a pervasive, financially savvy, and harmless instrument for evaluating the heart's electrical movement and is used for the distinguishing proof of cardiovascular diseases. This paper utilized deep learning ways to deal with four critical cardiovascular diseases: deviant heartbeat, myocardial localized necrosis, history of myocardial dead tissue, and ordinary people, using a public ECG pictures dataset of heart patients. The exchange learning approach was inspected using the low-scale pre-trained deep neural networks Squeeze Net and Alex Net. A novel convolutional neural network (CNN) engineering was presented for the expectation of heart irregularities. Third, the recently portrayed pre-trained models and our recommended CNN model filled in as element extraction apparatuses for standard machine learning algorithms, including support vector machine, K-nearest neighbours, decision tree, random forest, and Naïve Bayes. The exploratory outcomes demonstrate that the presentation measurements of the proposed CNN model outperform those of existing works, accomplishing 99.23% accuracy, 98.22% recall, 98.31% precision, and 98.21% F1 score. Moreover, the recommended CNN model achieves an ideal score of 99.79% for highlight extraction while utilising the NB algorithm.

**Impact Statement:** Artificial intelligence essentially improves personal satisfaction. In particular, the early ID of diseases can add to saving lives.

This review presents an original lightweight CNN engineering that upgrades the accuracy of cardiovascular disease order to 98.23% compared with present status of-the-craftsmanship techniques, using a dataset of ECG pictures from heart patients, and is operable on a solitary computer processor, subsequently tending to computational power limitations. The characterization accuracy has especially upgraded following the utilization of the proposed technique as an element extraction device for traditional machine learning methods. An accuracy of 99.79% has been achieved with the Naïve Bayes algorithm. Thus, this strategy may be integrated into the medical services IoT environment. This will spur further artificial intelligence specialists to examine elective methodologies for cardiovascular disease diagnosis.

**Index Terms:** Cardiovascular, deep learning, electrocardiogram (ECG) images, feature extraction, machine learning, transfer learning.

## I. INTRODUCTION

As per the World Wellbeing Association, cardiovascular diseases are the essential driver of mortality internationally. They are answerable for around 17.9 million fatalities every year, comprising 32% of worldwide mortality. Roughly 85% of all fatalities coming about because of cardiovascular disease are owing to coronary failures, clinically alluded to as myocardial areas of dead tissue (MI) [1]. A productive discovery of cardiovascular disease at a previous stage can

save a few lives [1]. Different methodologies are utilized in the medical services framework to distinguish heart problems, including electrocardiogram(ECG), echocardiography, cardiovascular attractive reverberation imaging, processed tomography, and blood testing. The ECG is a pervasive, smart, and harmless instrument for evaluating the heart's electrical movement [4]. It is used to determine cardiovascular disorders related to have the heart [4], [5]. A skilled clinician can distinguish heart ailment through ECG waves. This manual technique might yield incorrect discoveries and is tedious [5].

Progressions in artificial intelligence in healthcare hold huge potential to alleviate clinical blunders. In particular, the use of machine learning and deep learning systems for the computerised expectation of cardiovascular diseases. [3],[6]-[10]. Machine learning approaches require a specialist element for highlight extraction and choice to find appropriate elements before the characterization step. Highlight extraction is the most common way of reducing the quantity of elements in a dataset by changing or extending the information into a new, lower-layered highlight space while keeping the relevant data of the information [11], [12].

Highlight extraction includes producing another arrangement of elements, unmistakable from the information highlights, by consolidating unique elements into a lower-layered space that holds the larger part, while perhaps not all, of the data from the info information. The most perceived highlight extraction procedure is head part examination [13], [14]. Highlight choice is the most common way of wiping out unessential and excess elements (aspects) from the dataset during the preparation of machine learning algorithms. Include determination approaches can be arranged as solo, which don't need yield names, and managed, which use yield marks for highlight choice. Directed include choice envelops three techniques: the channel approach, the covering strategy, and the installing technique [11], [12].

Various machine learning techniques have been utilized to conjecture cardiovascular disorders. Soni et al. [15] compared several

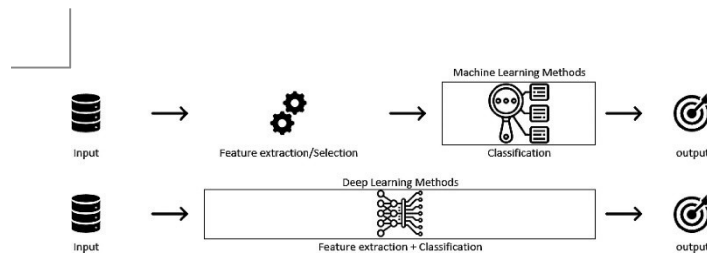


Fig. 1 Abstract concept of machine learning and deep learning.

Machine learning algorithms, including decision tree (DT), Naïve Bayes

(NB), K-Nearest Neighbours (K-NN), and Neural Network (NN), applied to the UCI Cleveland heart disease dataset. They discovered that DT displayed the most noteworthy accuracy at 89%. Dissanayake and Md Johar [16] inspected the effect of the component determination technique on machine learning for anticipating heart diseases utilizing the UCI Cleveland heart disease dataset. They broke down different component determination philosophies, including ANOVA, Chi-square, forward and in reverse choice, and Tether relapse. Accordingly, they utilized six machine learning classifiers: Decision Tree (DT), Random Forest (RF), Support Vector Machine (SVM), K-Nearest Neighbours (K-NN), Logistic Regression (LR), and Gaussian Naive Bayes (GNB). The element choice cycle improved forecast accuracy, accomplishing a most extreme grouping accuracy of 88.52% utilizing the DT classifier through the retrogressive component determination strategy. The use of machine learning methods, including Naive Bayes, Support Vector Machines, and Decision Trees, was analysed in [17] using ten times cross-approval on the South African coronary illness dataset containing 462 events. Naive Bayes (NB) yielded the most ideal results in heart disease detection, accomplishing an accuracy of 71.6%, sensitivity of 63%, and specificity of 76.16%. Kim et al.

[18] assessed the prescient adequacy of NN, SVM, CMAR, DT, and NB algorithms for cardiovascular diseases utilising two datasets: ultrasound pictures of carotid arteries (CAs) and heart rate variability (HRV) got from ECG signals. The incorporated extricated highlights from the CAs+ HRV dataset accomplished better precision thought about than the singular elements of CAs and HRV. Thusly, the SVM and CMAR classifiers outperformed the others with correctness of 89.51% and 89.46% separately.

On the other hand, deep learning, which is a subset of machine learning, freely distinguishes large features and patterns from datasets generated in the clustering step, eliminating the need for externalisation steps for light extraction and decision. Figure 1 illustrates the concept of machine learning and deep learning. In deep learning, a model is constructed by collecting hidden neural networks. Convolutional Neural Network (CNN) is an in-depth study that has produced commendable results in image

sequencing.

Deep learning and pre-trained organizations can work with include extraction without requiring the retraining of the whole organization, empowering move learning and arrangement [19]. This article utilizes pre-trained networks, explicitly Squeeze Net [20] and Alex Net [21], as an exchange learning methodology to assess their viability in heart disease characterization and as component extraction for traditional machine learning techniques in heart disease classification. Additionally, a clever CNN model is proposed for foreseeing heart diseases utilizing ECG pictures, which is utilized for highlight extraction of the ECG pictures following the preparation of the recently proposed CNN model.

The main contributions of this study are summarized as follows.

1. The main contributions of this study are summarized as follows.
2. The proposed CNN model achieves a success speed of 98.23%, which is best for learning on the continuous task [22] and inferior Squeeze Net and Alex Net, which came to 95.10%, 95.47%, and 96.79% difference.
3. This is, supposedly, the subsequent review using the ECG pictures dataset of heart patients [23], which might persuade different specialists to examine elective procedures for recognizing cardiovascular disorders with this dataset.
4. The transfer learning philosophy using Squeeze Net and Alex Net was inspected and stood out from the proposed model.
5. The pre-trained networks Squeeze Net, Alex Net, and our recommended CNN model filled in as element extractors to apply the extricated highlights to common machine learning methods: SVM, K-NN, DT, RF, and NB. The ideal results were achieved by our proposed CNN model for the NB algorithm, with an accuracy pace of 99.79% recorded.
6. The rest of this article is organized as follows. Segment II gives the writing audit. Segment III clarifies the techniques and the proposed CNN model utilized in this article. Area IV depicts the dataset and trial boundaries utilized. Area V presents the outcomes and conversations, while Segment VI completes the paper and offers future viewpoints.

## **II. RELATEDWORKS**

Various examinations [24]-[27] have been embraced to consequently anticipate cardiovascular diseases by machine learning and deep learning techniques, utilizing ECG information in computerized or picture designs.

Bharti et al. [28] assessed machine learning and deep learning techniques on the UCI heart disease dataset to foresee two categories. The deep learning algorithm achieved the best accuracy pace of 94.2%. The design of their deep

learning model has three completely associated layers: the main layer contains 128 neurons, prevailed by a dropout layer with a pace of 0.2; the subsequent layer comprises of 64 neurons, trailed by a dropout layer with a pace of 0.1; and the third layer includes 32 neurons. The ML procedures utilizing highlight determination and anomaly discovery achieved the accompanying accuracy rates: RF at 80.3%, LR at 83.31%, K- NN at 84.86%, SVM at 83.29%, DT at 82.33%, and XGBoost at 71.4%. The concentrate in [29] uncovered that deep learning is a more exact and helpful method for different clinical issues, including expectation. Deep learning strategies will displace customary ML dependent on include designing. Kiranyaz et al. [30] proposed a convolutional neural network (CNN) including three layers of a versatile execution of one-layered (1-D) convolutional layers. This organization was prepared on the MIT-BIH arrhythmia dataset to arrange broad ECG information streams. They accomplished accuracy paces of close to 100% and 97.6% in the grouping of ventricular ectopic beats and supraventricular ectopic beats, separately. The concentrate in [31] presented a CNN of three 1-D convolutional layers, three max-pooling layers, one completely associated layer, and one softmax layer. The channel aspects for the underlying two convolutional layers were laid out at 5, and a step of 2 was utilized for the initial two max-pooling layers. They accomplished a grouping accuracy of 92.7% for ECG pulses using the MIT-BIH arrhythmia dataset.

Khan et al. [22] utilized a transfer learning philosophy using the pre-trained single shot detector (SSD)- MobileNet-v2 [32] to recognize cardiovascular disease from an ECG pictures dataset of heart patients by foreseeing four heart irregularities: abnormal heartbeat (AH), myocardial infarction (MI), history of myocardial infarction (H.MI), and normal person (NP) classes. The text size was adjusted, and 12 angles of each ECG image were brightened as a preprocessing method. The SSD is used to analyse and characterize materials in the isolation phase. The data set was divided into 80% for training and 20% for testing. A batch size of 24, 200,000 preparation cycles and a learning speed of 0.0002 were used to solve the model. The preparation period stretched to about four days. An accuracy rate of 98.3% was obtained for the MI section.

Rahman et al. [33] introduced a deep CNN transfer learning philosophy to foresee Coronavirus and four critical heart inconsistencies using ECG pictures. The dataset had five classifications: Coronavirus, AH, MI, H. MI, and NP. Six unmistakable pre-trained deep convolutional neural network, in particular ResNet18, ResNet50, ResNet101, DenseNet201, inception V3, and MobileNet-v2, were utilized for characterization. Gamma revision, picture scaling, and z-score standardization were utilized as arrangement

strategies for the ECG pictures. Thusly, in two-class characterization (Coronavirus and ordinary) and three-class arrangement (Coronavirus, typical, and extra heart oddities), DenseNet201 outperformed different organizations with accuracy paces of 99.1% and 97.36%, separately. In the five-class order, Origin V3 outperformed different organizations with an accuracy of 97.83%.

Buddy et al. [36] presented a deep CNN transfer learning approach using pre-trained DenseNet for arrhythmia classifications (AH) got from ECG signals in the PTB and MIT-BIH arrhythmia datasets, which were changed into 2-D pictures. Due of the dataset's unevenness, an information increase strategy was executed. The DenseNet model was chosen because of its capacity to address the disappearing angle issue in deep organizations through the execution of thick associations among layers. Their model was assigned as CardioNet. The qualities for precision, recall, and F1 score were 98.62%, 98.68%, and 98.65%, separately.

Avanzato and Berritelli [37] presented a deep convolutional neural network consisting of four 1-D convolutional levels to predict three classifications of cardiovascular anomalies using ECG signals from the MIT-BIH arrhythmia dataset at each convolutional level cluster standardization level, rectified linear unit (ReLU) initial capacity, and was the maximum controlled pooling layer with a channel (bit) size of 4. The bottom convolutional layer had a channel size of 80, while subsequent layers used a channel size of 4.

This engineering utilized a normal pooling layer related to a softmax layer for grouping, as opposed to using totally associated layers. This model achieved an accuracy level of 98.33%.

They call Acharya. [38] fostered a deep convolutional neural network consisting of four-layer convolutional

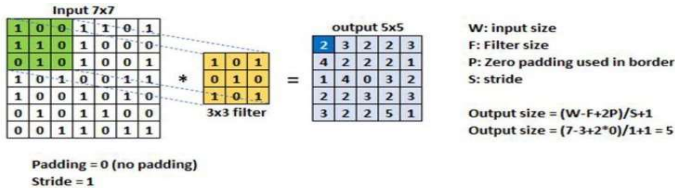


Fig. 2 Example of a convolution operation.

layers and three fully connected for myocardial localized lesion location using ECG signals from the PTB dataset. In this example, the cracked rectifier direct unit (Defective ReLU) is used, and the activation power layer. Each convolutional layer was a maximum pooling layer with channel size 2 and step 2. In that order, the channel sizes of the convolutional layers are 102, 24, 11, and 9. The

number of neurons in the fully connected layers is 30, 10, 2 different. A softmax layer followed the last fully connected layer. They obtained 93.53% and 95.22% general accuracy speeds for ECG shots with and without noise removal, respectively.

Naz and so on. [39] converted the ECG stimuli into  $32 \times 32$  pairs of images. Their method was tested using the MIT-BIH dataset with pre-trained CNN images Alex Net, VGG19, and Commencement V3 to predict myocardial infarction. The move gain was used to remove features from sample previously reared strains were included. As a result, SVM and K-NN features techniques were used for the parallel system. Using SVM, an accuracy of 97.60% was obtained.

### III. METHODS

#### A. Convolutional Neural Networks (CNN)

CNN is a special type of deep artificial neural network designed for image sequencing and processing in "deep learning". The information image measures  $227 \times 227 \times 3$ , which means that the width and height are 227 pixels, where the depth (path) is 3. An important capability of CNNs is to extract important points from the input image using sigmoid or softmax initialization capabilities to generate the expected Layer convolution method uses convolutional layers on the info information, using a channel or part to create a component map. Convolution is executed by traversing info across channel. Framework duplication is performed at each point, and so are the results. Component maps accumulate. Figure 2 illustrates the critical diagram of the convolution function for the depth contribution.

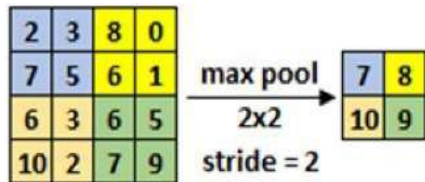


Fig. 3 Example of  $2 \times 2$  max-pooling with stride = 2.

The convolution cycle shows linearity. In order to detect nonlinearity and its consequences, the convolution layer is controlled by the actuation capacity level, e.g., ReLU or its variant. Following the convolution layer, the pooling layer, e.g. Figure 3 illustrates the critical diagram of maximum pooling for a single depth contribution.

#### B. Pre-trained Deep Learning Models

Pre-trained deep neural networks can work with transfer learning, highlight extraction, and arrangement. This article utilizes low-scaled SqueezeNet and AlexNet pre-trained CNN organizations, reasonable for execution on a solitary central processor, for transfer learning and component extraction. The transfer learning strategy is oftentimes utilized with pre-trained deep neural networks applied to a novel dataset. Thusly, it could get benefits from the pre-trained network that has gained a scope of properties adaptable to similar to occupations. Most pre-trained networks have been prepared on north of 1,000,000 photographs and can classify pictures into 1000 article types. In carrying out the transfer learning technique, the terminal layers of the pre-trained network are subbed with new layers to secure the unmistakable elements of the novel dataset. In this manner, the model goes through tweaking by being prepared on a novel dataset with characterized boundaries, trailed by an assessment of its exhibition on a different test dataset. Pre-trained deep neural networks can act as an element extraction instrument, killing the requirement for tedious preparation endeavors. This article uses highlights taken from pre trained organizations to prepare ordinary machine learning classifiers, including SVM, K-NN, DT, RF, and NB. The usage of pre-trained networks is clarified in the ensuing areas.

#### C. Proposed CNN Architecture

The proposed CNN model also contains six 2-D convolutional layers, three fully connected layers, three max pooling layers, eight faulty ReLU layers, eight group standardization layers, five dropout layers, depth connection layers two, and softmax layer the total number of elements is 38. The structure of the proposed model is shown in Figure 4.

The proposed CNN model has two branches that aim to include more representatives: the stack branch and the whole branch. The recommended CNN model requires a  $227 \times 227 \times 3$  dimensional information map. The info image enters two branches at the same time.

Stack part of three superimposed 2-D  $3 \times 3$  convolutional layers. Each of these two-layered convolution layers is dominated by a split ReLU layer and a group normalization layer.

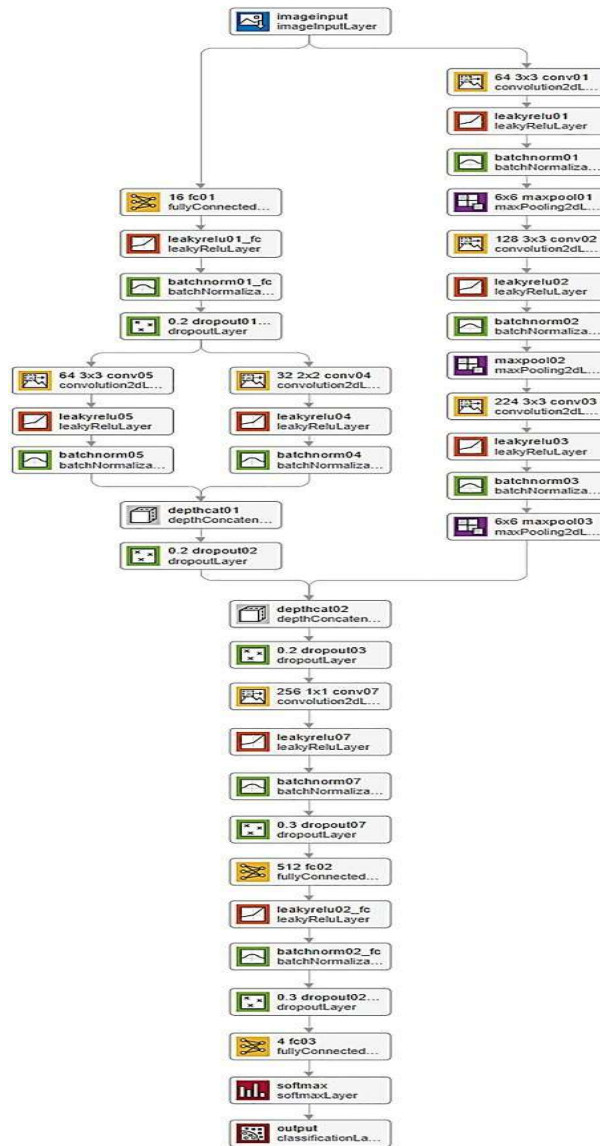


**Fig. 4 Representation architecture of the proposed CNN mod**

**TABLE I**

LAYERS ANALYSIS OF THE PROPOSED CNN MODEL

No.	Type	Name	Properties	Input size	Output size
1.	Image Input	Imageinput	-	227×227×3	227×227×3
2.	Convolution	conv01	64, 3x3, stride = 2, padding = same	227×227×3	114×114×64
3.	Max Pooling	maxpool01	6x6, stride = 3, padding = same	114×114×64	38×38×64
4.	Convolution	conv02	128, 3x3, stride = 2, padding = same	38×38×64	19×19×128
5.	Max Pooling	maxpool02	6x6, stride = 3, padding = same	19×19×128	7×7×128
6.	Convolution	conv03	224, 3x3, stride = 2, padding = same	7×7×128	4×4×224
7.	Max Pooling	maxpool03	6x6, stride = 3, padding = same	4×4×224	2×2×224
8.	Fully Connected	fc01	16	227×227×3	1×1×16
9.	Dropout	dropout01_fc	0.2	1×1×16	1×1×16
10.	Convolution	conv04	32, 2x2, stride = 1, padding = 1	1×1×16	2×2×32
11.	Convolution	conv05	64, 3x3, stride = 2, padding = 2	1×1×16	2×2×64
12.	Depth concatenation	depthcat01	Two inputs of size 2×2×32, 2x2x64		2×2×96
13.	Dropout	dropout02	0.2	2×2×96	2×2×96
14.	Depth concatenation	depthcat02	Two inputs of size 2×2×96, 2x2x224		2×2×320
15.	Dropout	dropout03	0.2	2×2×320	2×2×320
16.	Convolution	conv07	256, 1x1, stride = 1, padding = same	2×2×320	2×2×256
17.	Dropout	dropout07	0.3	2×2×256	2×2×256
18.	Fully Connected	fc02	512	2×2×256	1×1×512
19.	Dropout	dropout02_fc	0.3	1×1×512	1×1×512
20.	Fully Connected	fc03	4	1×1×512	1×1×4
21.	Softmax	Softmax	-	1x1x4	1x1x4
22.	Classification Output	Output	Cross-entropy as loss function	1x1x4	1x1x4

leaky ReLU: scale=0.1, batch normalization: Mean Decay=0.1, Variance Decay=0.1, Epsilon=0.00001, total number of learnable parameters=3430308

Stricter pooling layer. The LeakyReLU layer uses a leakyReLU rule capacity of size 0.1. Unlike ReLU, leakyReLU is slightly skewed in the negative position, which may preclude the issue of idle neurons [46]. The group normalization layer normalizes the inputs of each subgroup, serves to provide faster model preparation and improve accuracy. The maximum pooling layer implements the maximum pooling process on the component map by finding the strongest component in the location of the channel this directs the reduction of the spatial components of the element map, consequently comes with reducing the size of the boundaries and the computational cost of modelling. The recommended CNN model utilizes max-pooling layers with a channel size of 6×6 and a step of 3. This branch utilizes 64, 128, and 224 channels to remove deep elements from the information in the first, second, and third convolutional layers, separately. The result aspects at the finish of the stack branch are 2 × 2 × 224.

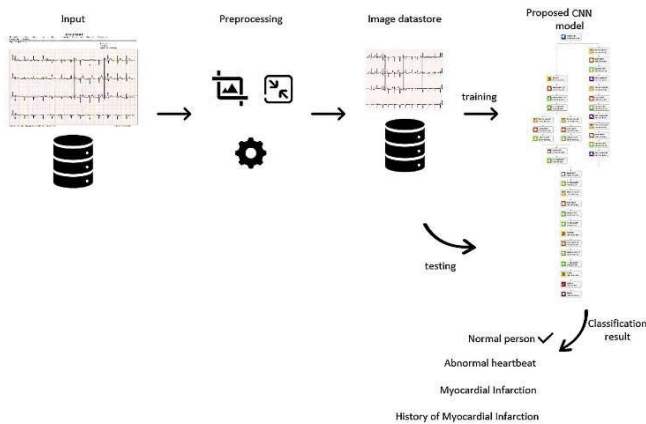
The underlying layer in the total engineering of our proposed CNN model is a totally associated layer, which is reflected in its assignment. In our idea, the totally associated layer contains 16 neurons. In any case, every node in the connecting layer is connected to every node in the first layer. This is the veining of the convolution layer in contrast to the former clear veins in which the convolutional channel segments are not set in stone While most of boundaries in the CNN start from the completely associated layers, the computational requests of the convolutional layer need altogether more noteworthy memory utilization. A completely associated layer is prevailed by a leakyReLU layer, a bunch convolutional layer, and a dropout layer, which moderate overfitting and improve the model's speculation limit.



Figure 4 outlines that the two convolutional layers, assigned as conv04 and conv05, are situated at a similar level resulting to the completely associated layer block to work with the extraction of greater elements.

Conv04 is a  $32 \times 2 \times 2$  convolutional layer with a step of 1 and cushioning of 1, while conv05 is a  $64 \times 3 \times 3$  convolutional layer with a step of 2 and cushioning of 2. The element maps from these two convolutional layers are connected to yield a component guide of aspects  $2 \times 2 \times 96$ . Following the connection of elements, a dropout layer is carried out to relieve the impact of connected includes and forestall overfitting.

The results delivered by the two branches are consolidated to frame a component guide of aspects  $2 \times 2 \times 320$ . A dropout layer is in this manner consolidated to moderate the model's overfitting. A  $1 \times 1$  convolutional layer with 256 channels is integrated to improve the model's nonlinearity and lessen the profundity or amount of component maps, consequently bringing down computational costs.



**Fig. 5.** Schematic of using the proposed CNN model for ECG images of cardiac patients' classification.

To improve the classification process, a fully connected layer consisting of 512 nodes is combined. The obtained results include a fully connected layer with four nodes, as determined by the number of clusters to be grouped, followed by a softmax layer to estimate the overall result.

Figure 5 shows the plan for utilizing the proposed CNN model to

characterize ECG pictures of heart patients. The provided photographs go through preprocessing by trimming, scaling, and expansion. The pre-processed

Preprocessing. As can be seen in Fig.6, the ECG images in the dataset contain Header and footer information that have no photographs are accordingly put away in the picture datastore. The proposed model is shown in Fig. 6 Samples from the electrocardiogram pictures dataset. (a) NP. (b) AH. (c) MI. (d)H. MI.

using the predetermined preparation boundaries and the ECG pictures contained in the picture datastore. The model gains elements and alters its movable boundaries in like manner. Endless supply of preparing, the model is ready to assess ECG pictures for the grouping of cardiovascular oddities into one of four classifications: NP, AH, MI, and H.

### III. EXPERIMENTS

#### A. ECG Images Dataset of Cardiac Patients

The predetermined methodologies were assessed on the ECG Pictures dataset of cardiovascular patients [23]. This dataset has 928 particular patient records ordered into four kinds, as outlined in Table II. The four classes are NP, AH, MI, and H. Figure 6 delineates a few examples from the dataset. An NP is a person healthy with no heart issues. An arrhythmia happens when the heart's electrical driving forces are exorbitantly fast, unnecessarily sluggish, or sporadic, bringing about an unpredictable heartbeat. Myocardial dead tissue, usually referred to as cardiovascular failure, happens when the blood stream in the coronary conduit reduces or stops, bringing about injury to the heart muscle. The people with an H. MI have of late recovered from myocardial localized necrosis or respiratory failure.

#### B. Experimental Settings

TABLE II  
PUBLIC ECG IMAGES DATASET DESCRIPTION

No.	Class	Number of images
1.	Normal person	284
2.	Abnormal Heartbeat	233
3.	Myocardial Infarction	239
4.	History of Myocardial Infarction	172
Total		928

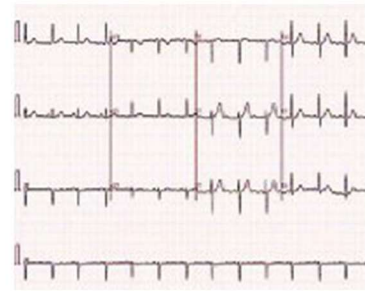
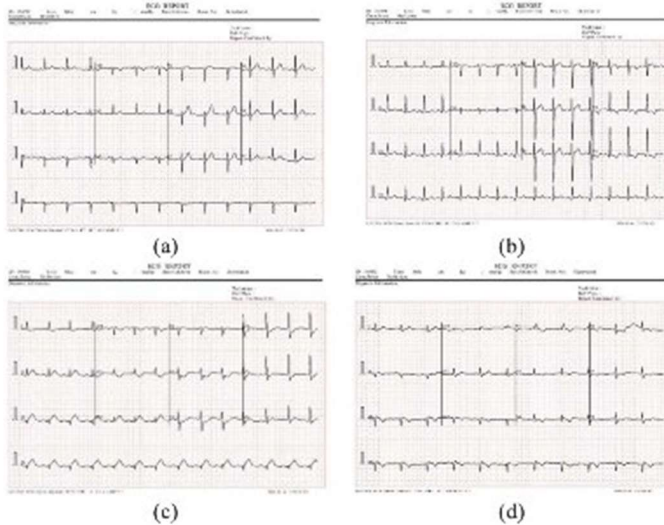


Fig. 7. Sample from the ECG images dataset after performing cropping as a preprocessing.

TABLE III  
TRAINING PARAMETERS AND VALUES FOR DEEP LEARNING METHODS

Optimizer	Weight Initializer	Bias Initializer	L2 Regularization	Epochs no.	Mini-Batch Size
Adam	Xavier	Zeros	0.0001	16	128

a 4 GB NVIDIA GeForce 820M GPU<sup>1</sup> and running Windows 10 Pro 64-b.

relation to the features we need. Therefore, we have applied

The examinations used MATLAB 2021b on an Intel Center i7-4510U computer processor working at 2.00 GHz with 8GB of RAM, and all photographs were trimmed to underscore the huge highlights, as represented in Fig. 7. Moreover, all ECG pictures were scaled to a uniform goal of 227×227 with three channels (RGB) before model preparation.

Information increase. Information increase was utilized on the dataset [47] to improve the heartiness and exactness of the made model. It upgrades the dataset's picture amount and mitigates the results of preparing the model on an

imbalanced dataset. Three increase strategies—revolution, flipping, and interpretation—were utilized on the predetermined dataset [48]. This increased the assortment to a sum of 4,700 photographs.

Boundaries for deep getting the hang of preparing. Because of the computational power of hyperparameter improvement, all preliminaries used the preparation settings determined in Table III. The Adam enhancer is used to prepare the model for 16 ages with a minibatch size of 128. By the by, considering that the underlying learning rate (LR) is the principal hyperparameter, a few LR values were utilized in the preliminaries, as point by point in the ensuing segment. In light of these settings, the cycles per age absolute 29, and the all-out emphases for model preparation add up to 464. Fivefold cross-approval was utilized to accomplish solid outcomes in testing and assessing the model. The dataset is divided into five portions, with four fragments dispensed for preparing and one section assigned for testing (3760 pictures for preparing and 940 pictures for testing).

Subsequently, five significant contrasts among preparing and testing were executed. The results are the mean of the five folds.

Its compute capability is 2.1 and it is not supported by MATLAB 2021b. Hence, all experiments were run on a single CPU.

TABLE IV

PERFORMANCE MEASURES

Measures	Defined as	
Accuracy	$(TP+TN)/(TP+FP+FN+TN)$	(1)
Recall	$TP/(TP+FN)$	(2)
Precision	$TP/(TP+FP)$	(3)
F1 score	$(2 \times Recall \times Precision)/(Recall+Precision)$	(4)

TABLE V  
NETWORKS PROPERTIES<sup>2</sup>

Network	Depth	No. of Layers	No. of Connections	No. of Parameters (million)
SqueezeNet	18	68	75	1.24
AlexNet	8	25	24	61.0
Proposed CNN	6	38	39	3.43

For all networks, input image size is 227×227×3.

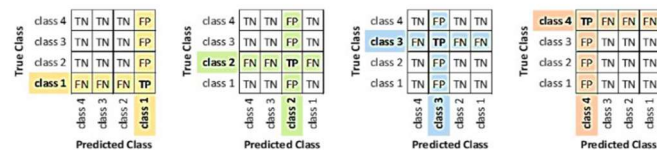


Fig. 8. Semantic of the confusion matrices for four class’s results.

## V. RESULTS AND DISCUSSIONS

Accuracy, precision, recall, F1 score, and training and testing lengths were utilized for execution investigation. The estimations get from the assessment of information inside a disarray framework. Table V outlines the meanings of the

measurements got from the disarray matrix. Accuracy is both the range of parameters and the number of parameters expected as a judge, communicated as a quantity. Memory refers to the extent to which accurately anticipated positive intentions are theoretically complete in the actual positive category. Precision refers to the extent to which expected positive mood accuracy deviates from mood in the predicted positive category. The F1 score satisfies the weighted normal of Recall and Precision. Thus, it involves both false negative values and false positive thinking.

Figure 8 outlines the semantics of the disarray lattice for four-class datasets, explicitly the ECG pictures dataset of heart patients. The exploratory exhibition measurements are gotten from the situations introduced in Table IV.

A. Results of Transfer Learning and Proposed CNN Model

The high-level plans of the pre-trained networks Squeeze Net and Alex Net were utilized to carry out the transfer learning philosophy in our exploration. Both were at first prepared for the arrangement of 1000 picture classes. To adjust these organizations for distinguishing the new assortment of ECG pictures in the dataset, we alter the last layers of these models to line up with the new errand. In Alex Net, the last completely associated layer is subbed by another completely associated layer of indistinguishable aspects.

Here, the total number of layers in the network was counted, not even the convolutional layers and dense layers.

**TABLE VI**

CALCULATED PERFORMANCE MEASUREMENTS FOR SQUEEZE-NET, ALEXNET, AND THE PROPOSED CNN MODEL FOR DIFFERENT LR VALUES

Model	LR	A. (%)	R. (%)	P. (%)	F1 (%)	T1 (m)	T2 (m)
Squeeze-Net (Transfer learning)	0.01	24.79	25.00	NaN	NaN	245.0	2.3
	0.001	24.15	25.00	NaN	NaN	212.7	2.1
	0.0001	95.47	95.43	96.07	95.40	219.9	2.2
AlexNet (Transfer learning)	0.01	24.15	25.00	NaN	NaN	198.9	2.1
	0.001	37.00	37.88	NaN	NaN	209.5	2.1
	0.0001	96.79	96.80	97.02	96.78	199.5	2.1
Proposed CNN	0.01	97.24	97.24	97.31	97.22	<b>189.4</b>	<b>2.0</b>
	0.001	97.89	97.89	97.97	97.88	190.0	2.1
	0.0001	<b>98.23</b>	<b>98.22</b>	<b>98.31</b>	<b>98.21</b>	190.7	<b>2.0</b>

LR: initial learning rate, A.: accuracy, R.: recall, P.: precision, F1: F1 score, T1: training time, T2: testing time.

The bold values indicate the best results. **TABLE VII**

PERFORMANCE MEASUREMENTS VALUES OBTAINED FOR EACH FOLD OF THE PROPOSED MODEL

LR	Folds	A. (%)	R. (%)	P. (%)	F1 (%)	T1 (m)	T2 (m)
0.01	Fold-1	97.77	97.75	97.83	97.73	200.23	2.05
	Fold-2	97.87	97.86	97.89	97.86	185.88	2.00
	Fold-3	95.43	95.48	95.57	95.39	185.08	1.97
	Fold-4	97.13	97.11	97.26	97.11	184.67	2.05
	Fold-5	97.98	97.98	98.02	97.99	191.00	1.98
	<b>Average</b>		<b>97.24</b>	<b>97.24</b>	<b>97.31</b>	<b>97.22</b>	<b>189.37</b>
0.001	Fold-1	99.15	99.15	99.15	99.15	187.52	2.01
	Fold-2	98.19	98.18	98.23	98.16	191.57	2.08
	Fold-3	95.96	95.99	96.14	95.94	190.17	2.10
	Fold-4	97.66	97.64	97.80	97.63	185.62	2.16
	Fold-5	98.51	98.50	98.55	98.51	194.87	1.99
	<b>Average</b>		<b>97.89</b>	<b>97.89</b>	<b>97.97</b>	<b>97.88</b>	<b>189.95</b>
0.0001	Fold-1	99.47	99.46	99.47	99.46	195.12	2.03
	Fold-2	97.66	97.64	97.74	97.61	185.85	2.00
	Fold-3	97.55	97.53	97.74	97.54	187.72	2.00
	Fold-4	98.30	98.28	98.33	98.27	196.80	2.01
	Fold-5	98.19	98.18	98.28	98.17	187.92	1.99
	<b>Average</b>		<b>98.23</b>	<b>98.22</b>	<b>98.31</b>	<b>98.21</b>	<b>190.68</b>

The bold values indicate the average of the five folds.

The size of the neurons is related to the size of our expected clusters, apparently four. Since SqueezeNet completely removes overlapping layers, we replace a final convolutional layer, which distinguishes 1000 classes, with another convolutional layer using  $4 \times 1 \times 1$  channels. In the two pre-trained grids which is used, a new system layer is populated for the previous one, resulting in terms of probabilities registered by the softmax layer. Objects in the network are previously trained in and our proposed CNN is introduced in Table V.

Table VI presents the performance measures of the pre-trained models (SqueezeNet and AlexNet) used in the change learning philosophy, which are close to our proposed CNN model for the ECG image dataset. Specific learning rate (LR) values were used for each sample: 0.01, 0.001, and 0.0001. The most effective improvement rate, with a specific accuracy of 98.23%, was achieved by our proposed CNN model at a learning speed of 0.0001. Table VII presents the complete evaluation of the proposed model.

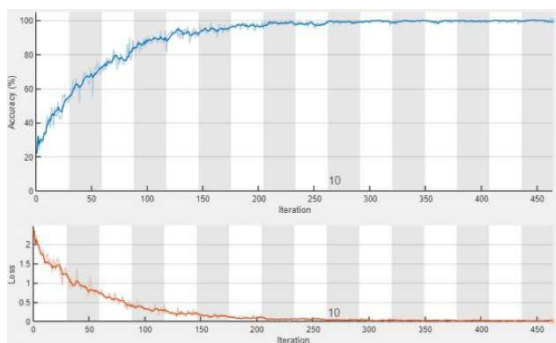


Fig. 9. Training Progress for our proposed CNN model on the ECG images dataset in fold-1 (LR: 0.0001 and other hyperparameters are as in Table III).

**TABLE VIII**

MODELS COMPARISON

Model	Average Accuracy (%)				
	NP	AH	MI	H. MI	Average
Work in [22]	93.7	93.6	96.2	96.8	95.1
Proposed CNN	99.8	93.1	100.0	99.9	98.2
	Average Precision (%)				
	NP	AH	MI	H. MI	Average
Work in [22]	96.2	97.2	98.3	98.3	97.5
Proposed CNN	97.4	100.0	99.4	96.5	98.3

NP: normal person, AH: abnormal heartbeat, MI: myocardial infarction, H.MI: history of myocardial Infarction classes.

The typical accuracy rate for the proposed CNN model shows reliably high outcomes notwithstanding varieties in the RL values. On the other hand, the pre-trained SqueezeNet and AlexNet models exhibit less than ideal execution at transfer learning paces of 0.01 and 0.001, despite the fact that give barely further developed results while the learning rate is changed in accordance with 0.0001. This is because of the way that, in move learning, the loads of pre-trained models are not procured starting from the earliest stage. Subsequently, to forestall entanglement in nearby minima, it is fitting to start with a lower learning rate, for example, 0.0001, while utilizing move learning systems.

The typical accuracy rates are 96.79% for AlexNet and 95.43% for SqueezeNet, with a learning rate of 0.0001. Alternately, the proposed CNN model exhibits better execution analysed than different models with respect to time proficiency, as outlined in Table VI. Notwithstanding SqueezeNet having the least boundaries and being a completely convolutional network, it has the most unfortunate outcomes with respect to time effectiveness. The broad algorithms in the convolutional layers bring about delayed handling times, especially when executed on a solitary computer processor stage.

Figure 9 delineates the preparation progression of our proposed CNN model on the ECG pictures dataset in overlap 1 (learning rate = 0.0001). The accuracy rate logically improves with each ensuing reiteration.

Besides, the misfortune decreases step by step as the cycle propels, at last coming to 0.0043.

The disarray frameworks created for each overlay following the preparation of our proposed CNN models with a learning pace of 0.0001 on the ECG pictures dataset are shown in Fig. 10.

As far as anyone is concerned, the sole distribution in the writing that uses the indistinguishable data and arranges the four classes is the review

referred to in [22], which has been tended to in Segment II. The dataset was partitioned into 80% for training and 20% for testing in [22].

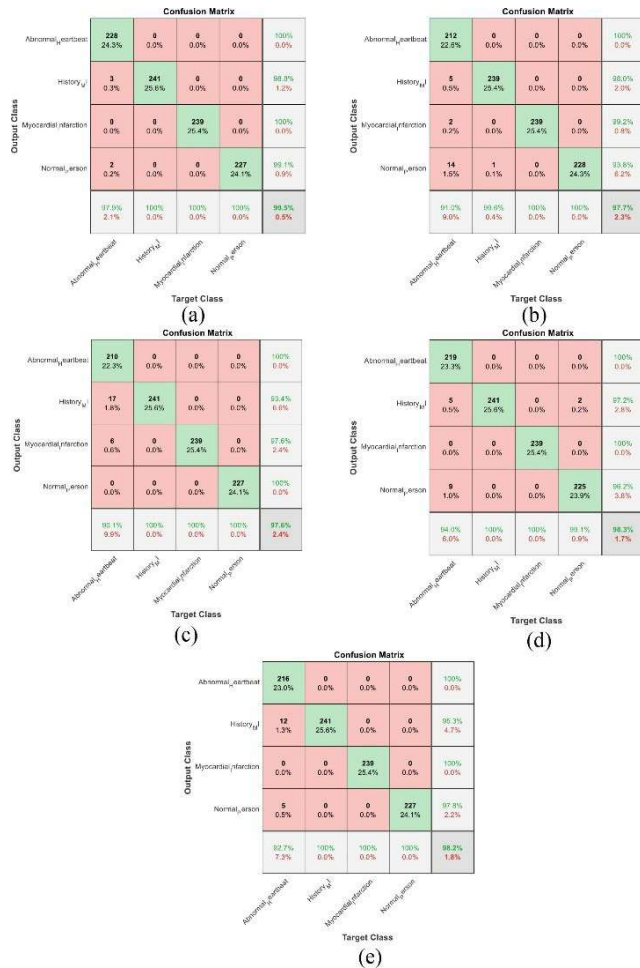


Fig. 10. Confusion matrices of the proposed CNN model for classification of heart diseases in the ECG images dataset for each fold (RL: 0.0001 and other hyper-parameters are as in Table III).

**TABLE IX**  
PROPERTIES OF THE EXTRACTED FEATURES FROM PRE-TRAINED NETWORKS

Pretrained Network	Training features size	Testing features size	Time taken (m)	Activation Feature Layer
SqueezeNet	3760x196000	940x196000	13.37	conv10 (64)
AlexNet	3760x4096	940x4096	11.24	fc7 (20)
Proposed CNN	3760x512	940x512	10.77	fc02 (32)

The model was prepared with a group size of 24 and a learning rate of 0.0002. Their preparation span broadened almost four days. Their distribution demonstrates a precision rate of 98.3% for class MI, but our proposed CNN model outperforms this with an accuracy pace of 99.4% for a similar class. Table VIII compares the discoveries from [22], where the accuracy paces of each class were gotten from their disarray network, with our proposed CNN model.

B. Results of Using Pre-trained Deep Learning Models As a Feature Extractor.

The pre-trained SqueezeNet and AlexNet networks were used to extract the features of the ECG images in the

dataset. Aswell

TABLE X

CALCULATED PERFORMANCE MEASUREMENTS FOR MACHINE LEARNING ALGORITHMS THAT USE PRE-TRAINED NETWORKS SQUEEZENET, ALEXNET, AND PROPOSED CNN AS FEATURES EXTRACTOR APPLIED ON ECG IMAGES DATASET

Pretrained Network	Algorithm	Accuracy (%)	Recall (%)	Precision (%)	F1 score (%)	Training Time (s)	Testing Time (s)
SqueezeNet	SVM	97.87	97.85	97.95	97.84	642.44	10.37
	K-NN	85.00	84.88	86.20	84.53	24.19	611.49
	DT	89.15	89.04	88.98	88.70	2159.1	1.15
	RF	98.94	98.93	98.95	98.92	7508.6	6.85
	NB	73.94	74.12	75.64	74.05	1245.7	39.75
AlexNet	SVM	97.66	97.64	97.79	97.64	6.3357	0.2333
	K-NN	90.32	90.18	91.13	90.17	1.0016	9.2097
	DT	91.38	91.29	91.43	91.19	11.8865	0.0656
	RF	97.55	97.53	97.66	97.51	24.3221	0.3720
	NB	72.02	72.18	73.31	71.89	2.6253	0.5649
Proposed CNN	SVM	99.47	99.46	99.47	99.46	<b>0.2858</b>	0.0372
	K-NN	99.68	99.68	99.68	99.68	1.6159	1.4100
	DT	99.04	99.03	99.05	99.03	0.3292	<b>0.0129</b>
	RF	99.57	99.57	99.58	99.57	3.3505	0.1597
	NB	<b>99.79</b>	<b>99.79</b>	<b>99.78</b>	<b>99.78</b>	0.4129	0.1163

*The bold values indicate the best results.*

The pre-trained SqueezeNet and AlexNet models were utilized to separate highlights from the ECG pictures in the dataset. Moreover, our proposed CNN model filled in as an element extractor, and the results were looked at. Deep learning's capacity takes into consideration the extraction of picture highlights without requiring the re-preparing of the whole organization. The organizations not entirely settled through the forward spread of information pictures to the assigned component layer. The initiation include layers used are conv10 (layer 64), fc7 (layer 20), and fc02 (layer 32) for SqueezeNet, AlexNet, and our proposed CNN model, separately. Table IX outlines the properties of the recovered highlights. The recovered highlights were used to prepare the machine learning algorithms: SVM, k-NN, DT, RF, and NB.

The presentation measurements are figured and shown in Table X. The best result was accomplished with an accuracy, recall, precision, and F1- score of 99.79% involving the NB strategy related to our recommended CNN model as the component extractor. The SVM algorithm accomplished accuracy paces of 99.47%, 97.87%, and 97.66% while using our recommended CNN model, SqueezeNet, and AlexNet, individually, for highlight extraction. The ideal outcomes for all exhibition measurements were accomplished using our proposed CNN model as the element extractor. In the examination of SqueezeNet and AlexNet, we almost accomplished unrivaled accuracy rates for the SVM, RF, and NB algorithms using highlights removed from SqueezeNet contrasted with those got from AlexNet. In any case, the preparation and testing lengths for SqueezeNet-based strategies were stretched out attributable to the expanded measure of the removed elements. Regardless of having the littlest separated highlight size, our recommended CNN model achieved prevalent outcomes across all exhibition measurements, as shown in Table X. This shows that our proposed model is intended to become familiar with the fundamental parts of the ECG pictures dataset.

Subsequently, the recommended model offers unrivaled accuracy rates as



well as decreased computational costs compared with existing writing. The proposed model could yield further developed results assuming enhancement algorithms are utilized to find out the upsides of its hyperparameters.

## VI. CONCLUSION

This examination presents a lightweight CNN-based model for ordering four head cardiovascular irregularities: AH, MI, H. MI, and NP, using a public ECG picture dataset of heart patients. The exploratory outcomes demonstrate that the proposed CNN model achieves extraordinary execution in cardiovascular disease order and can additionally act as an element extraction device for customary machine learning classifiers.

The recommended CNN model fills in as a helper apparatus for doctors in the clinical space to recognize heart disease from ECG pictures, subsequently evading the human technique that outcomes in mistakes and postponements.

In future exploration, enhancement methods might be utilized to determine ideal qualities for the hyperparameters of the proposed CNN model. The

proposed approach can likewise be used for anticipating a few different kinds of issues. The recommended model is ordered as a low-scale deep learning technique in view of its number of layers, boundaries, and profundity. Thus, a study on the applicability of the proposed model for segmentation in today's online landscape can be explored

## REFERENCE

1. World Health Organization (WHO), *Cardiovascular diseases*, Jun. 11, 2021. Accessed: Dec. 27, 2021. [Online]. Available: <https://www.who.int/health-topics/cardiovascular-diseases>
2. Government of Westren Australia, Department of Health, *Common medical tests to diagnose heart conditions*, Accessed: Dec. 29, 2021. [Online]. Available: [https://www.health.wa.gov.au/Articles/A\\_E/Common-medical-tests-to-diagnose-heart-conditions](https://www.health.wa.gov.au/Articles/A_E/Common-medical-tests-to-diagnose-heart-conditions)
3. M. Swathy and K. Saruladha, A comparative study of classification and prediction of cardio-vascular diseases (CVD) using machine learning and deep learning techniques, ICT Exp., to be published, 2021. [Online]. Available: <https://doi.org/10.1016/j.ict.2021.08.021>
4. R. R. Lopes et al., Improving electrocardiogram-based detection of rare genetic heart disease using transfer learning: An application to phospholamban p.Arg14del mutation carriers, *Comput. Biol. Med.*, vol. 131, 2021, Art. no. 104262. [Online]. Available: <https://doi.org/10.1016/j.combiomed.2021.104262>
5. R. J. Martis, U. R. Acharya, and H. Adeli, Current methods in electrocardiogram characterization, *Comput. Biol. Med.*, vol. 48, pp. 133–149, 2014. [Online]. Available: <https://doi.org/10.1016/j.combiomed.2014>
6. A. Rath, D. Mishra, G. Panda, and S. C. Satapathy, Heart disease detection using deep learning methods from imbalanced ECG samples, *Biomed. Signal Process. Control*, vol. 68, 2021, Art. no. 102820. [Online]. Available: <https://doi.org/10.1016/j.bspc.2021.102820>
7. A. Mincholé and B. Rodriguez, Artificial intelligence for the electrocardiogram, *Nature Med.*, vol. 25, no. 1, pp. 22–23, 2019. [Online]. Available: <https://doi.org/10.1038/s41591-018-0306-1>
8. A. Isin and S. Ozdalili, Cardiac arrhythmia detection using deep learning, *Procedia Comput. Sci.*, vol. 120, pp. 268–275, 2017. [Online]. Available: <https://doi.org/10.1016/j.procs.2017.11.238>
9. H. Bleijendaal et al., Computer versus cardiologist: Is a machine learning algorithm able to outperform an expert in diagnosing phospholamban (PLN) p.Arg14del mutation on ECG?, *Heart Rhythm*, vol. 18, no. 1, pp. 79–87, 2020. [Online]. Available: <https://doi.org/10.1016/j.hrthm.2020.08.021>
10. U. R. Acharya, H. Fujita, O. S. Lih, M. Adam, J. H. Tan, and C. K. Chua, Automated detection of coronary artery disease using different durations of ECG segments with convolutional neural network, *Knowl.-Based Syst.*, vol.

- 132, pp. 62–71, 2017. [Online]. Available: <https://doi.org/10.1016/j.knosys.2017.06.003>
11. M. Kantardzic, *Data Mining: Concepts, Models, Methods, and Algorithms*, 3rd ed. Hoboken, NJ, USA: Wiley, 2020.
12. S. García, J. Luengo, and F. Herrera, *Data Preprocessing in Data Mining*, 1st ed. Berlin, Germany: Springer, 2015.
13. G. Dougherty, *Pattern Recognition and Classification: An Introduction*. Berlin, Germany: Springer, 2013.
14. A. Subasi, *Practical Machine Learning for Data Analysis Using Python*. Cambridge, MA, USA: Academic, 2020.
15. J. Soni, U. Ansari, D. Sharma, and S. Soni, Predictive data mining for medical diagnosis: An overview of heart disease prediction, *Int. J. Comput. Appl.*, vol. 17, no. 8, pp. 43–48, 2011.
16. K. Dissanayake and M. G. MdJohar, Comparative study on heart disease prediction using feature selection techniques on classification algorithms, *Appl. Comput. Intell. Soft Comput.*, vol. 2021, 2021, Art. no. 5581806. [Online]. Available: <https://doi.org/10.1155/2021/5581806>
17. A. H. Gonsalves, F. Thabtah, R. M. A. Mohammad, and G. Singh, Prediction of coronary heart disease using machine learning: An experimental analysis, in *Proc. 3rd Int. Conf. Deep Learn. Technol.*, 2019, pp. 51–56. [Online]. Available: <https://doi.org/10.1145/3342999.3343015>
18. H. Kim, M. I. M. Ishag, M. Piao, T. Kwon, and K. H. Ryu, A data mining approach for cardiovascular disease diagnosis using heart rate variability and images of carotid arteries, *Symmetry*, vol. 8, no. 6, 2016, Art. no. 47. [Online]. Available: <https://doi.org/10.3390/sym8060047>
19. T. Ozcan, A new composite approach for COVID-19 detection in X-ray images, *Appl. Soft Comput.*, vol. 111, 2021, Art. no. 107669. [Online]. Available: <https://doi.org/10.1016/j.asoc.2021.107669>
20. F. N. Iandola, S. Han, M. W. Moskewicz, K. Ashraf, W. J. Dally, and K. Keutzer, SqueezeNet: Alexnet-level accuracy with 50x fewer parameters and < 0.5 MB model size, 2016, arXiv:1602.07360.
21. A. Krizhevsky, I. Sutskever, and G. E. Hinton, Imagenet classification with deep convolutional neural networks, *Adv. Neural Inf. Process. Syst.*, vol. 25, pp. 1097–1105, 2012.
22. A. H. Khan, M. Hussain, and M. K. Malik, Cardiac disorder classification by electrocardiograms sensing using deep neural network, *Complexity*, vol. 2021, 2021, Art. no. 5512243. [Online]. Available: <https://doi.org/10.1155/2021/5512243>
23. A. H. Khan and M. Hussain, ECG images dataset of cardiac patients, *Mendeley Data*, vol. V2, 2021. [Online]. Available: <https://doi.org/10.17632/gwbz3fsgp8.2>
24. C. Potes, P. Saman, A. Rahman, and B. Conroy, Ensemble of feature-based and deep learning-based classifiers for detection of abnormal heart sounds, in *Proc. Comput. Cardiol. Conf.*, 2016, pp. 621–624.
25. A. Nannavecchia, F. Girardi, P. R. Fina, M. Scalera, and G. Dimauro, Personal heart health monitoring based on 1D convolutional neural network, *J. Imag.*, vol. 7, no. 2, 2021, Art. no. 26. [Online]. Available: <https://doi.org/10.3390/ijimaging7020026>
26. Q. Zhang, D. Zhou, and X. Zeng, HeartID: A multiresolution convolutional neural network for ECG-based biometric human identification in smart health applications, *IEEE Access*, vol. 5, pp. 11805–11816, 2017. [Online]. Available: <https://doi.org/10.1109/ACCESS.2017.2707460>
27. U. R. Acharya, S. L. Oh, Y. Hagiwara, J. H. Tan, M. Adam, and R. S. Tan, A deep convolutional neural network model to classify heartbeats, *Comput. Biol. Med.*, vol. 89, pp. 389–396, 2017. [Online]. Available: <https://doi.org/10.1016/j.compbiomed.2017.08.022>
28. R. Bharti, A. Khamparia, M. Shabaz, G. Dhiman, S. Pande, and P. Singh, Prediction of heart disease using a combination of machine learning and deep learning, *Comput. Intell. Neurosci.*, vol. 2021, 2021, Art. no. 8387680. [Online]. Available: <https://doi.org/10.1155/2021/8387680>
29. P. Bizopoulos and D. Koutsouris, Deep learning in cardiology, *IEEE Rev. Biomed. Eng.*, vol. 12, pp. 168–193, 2018. [Online]. Available: <https://doi.org/10.1109/RBME.2018.2885714>

30. S. Kiranyaz, T. Ince, and M. Gabbouj, Real-time patient-specific ECG classification by 1-D convolutional neural networks, *IEEE Trans. Biomed. Eng.*, vol. 63, no. 3, pp. 664–675, Mar. 2016. [Online]. Available: <https://doi.org/10.1109/TBME.2015.2468589>
31. M. Zubair, J. Kim, and C. Yoon, An automated ECG beat classification system using convolutional neural networks, in *Proc. 6th Int. Conf. IT Convergence Secur.*, 2016, pp. 1–5. [Online]. Available: <https://doi.org/10.1109/ICITCS.2016.7740310>
32. M. Sandler, A. Howard, M. Zhu, A. Zhmoginov, and L.-C. Chen, Mobilenetv2: Inverted residuals and linear bottlenecks, in *Proc. IEEE Conf. Comput. Vis. Pattern Recognit.*, 2018, pp. 4510–4520.
33. T. Rahman et al., COV-ECGNET: COVID-19 detection using ECG trace images with deep convolutional neural network, 2021, arXiv:2106.00436.
34. G. Huang, Z. Liu, L. V. D. Maaten, and K. Q. Weinberger, Densely connected convolutional networks, in *Proc. IEEE Conf. Comput. Vis. Pattern Recognit.*, 2017, pp. 2261–2269.
35. C. Szegedy, V. Vanhoucke, S. Ioffe, J. Shlens, and Z. Wojna, Rethinking the inception architecture for computer vision, in *Proc. IEEE Conf. Comput. Vis. Pattern Recognit.*, 2016, pp. 2818–2826.
36. A. Pal, R. Srivastava, and Y. N. Singh, CardioNet: An efficient ECG arrhythmia classification system using transfer learning, *Big Data Res.*, vol. 26, 2021, Art. no. 100271. [Online]. Available: <https://doi.org/10.1016/j.bdr.2021.100271>
37. R. Avanzato and F. Beritelli, Automatic ECG diagnosis using convolutional neural network, *Electronics*, vol. 9, no. 6, 2020, Art. no. 951. [Online]. Available: <https://doi.org/10.3390/electronics9060951>
38. U. R. Acharya, H. Fujita, S. L. Oh, Y. Hagiwara, J. H. Tan, and M. Adam, Application of deep convolutional neural network for automated detection of myocardial infarction using ECG signals, *Inf. Sci.*, vol. 415–416, pp. 190–198, 2017. [Online]. Available: <https://doi.org/10.1016/j.ins.2017.06.027>
39. M. Naz, J. H. Shah, M. A. Khan, M. Sharif, M. Raza, and R. Damaševičius, From ECG signals to images: A transformation based approach for deep learning, *PeerJ Comput. Sci.*, vol. 7, 2021, Art. no. e386, doi: [10.7717/peerj-cs.386](https://doi.org/10.7717/peerj-cs.386).
40. H. El-Amir and M. Hamdy, *Deep Learning Pipeline: Building a Deep Learning Model With TensorFlow*. New York, NY, USA: Apress Media, 2020.
41. M. A. Hearst, S. T. Dumais, E. Osuna, J. Platt, and B. Scholkopf, Support vector machines, *IEEE Intell. Syst. Appl.*, vol. 13, no. 4, pp. 18–28, Apr. 1998. [Online]. Available: <https://doi.org/10.1109/5254.708428>
42. M. Abubaker and W. M. Ashour, Efficient data clustering algorithms: Improvement over Kmeans, *Int. J. Intell. Syst. Appl.*, vol. 5, no. 3, pp. 37–49, 2013. [Online]. Available: <https://doi.org/10.5815/ijisa.2013.03.04>
43. B. Charbuty and A. Abdulazeez, Classification based on decision tree algorithm for machine learning, *J. Appl. Sci. Technol. Trends*, vol. 2, no. 1, pp. 20–28, 2021.
44. L. Breiman, Random forests, *Mach. Learn.*, vol. 45, no. 1, pp. 5–32, 2001. [Online]. Available: <https://doi.org/10.1023/A:1010933404324>
45. E. Miranda, E. Irwansyah, A. Y. Amelga, M. M. Maribondang, and M. Salim, Detection of cardiovascular disease risk level for adults using naive Bayes classifier, *Healthcare Inform. Res.*, vol. 22, no. 3, pp. 196–205, 2016. [Online]. Available: <https://doi.org/10.4258/hir.2016.22.3.196>
46. G. Masetti and F. D. Giandomenico, Analyzing forward robustness of feedforward deep neural networks with LeakyReLU activation function through symbolic propagation, in *Proc. Joint Eur. Conf. Mach. Learn. Knowl. Discov. Databases*, 2020, pp. 460–474.
47. S. Shahinfar, P. Meek, and G. Falzon, How many images do I need? Understanding how sample size per class affects deep learning model performance metrics for balanced designs in autonomous wildlife monitoring, *Ecological Inform.*, vol. 57, 2020, Art. no. 101085. [Online]. Available: <https://doi.org/10.1016/j.ecoinf.2020.101085>
48. B. Zoph, E. D. Cubuk, G. Ghiasi, T. Lin, J. Shlens, and Q. V. Le, Learning data augmentation strategies for object detection, in *Proc. Eur. Conf. Comput. Vis.*, 2020, pp. 566–583.